

# Characteristic length scale in cleavage cracking across high-angle grain boundary

Jin Chen, Yu Qiao \*

*Department of Structural Engineering, University of California – San Diego, La Jolla, CA 92093-0085, USA*

Received 2 August 2007; received in revised form 26 September 2007; accepted 1 October 2007

Available online 12 November 2007

## Abstract

The factors that govern cleavage cracking across high-angle grain boundaries are investigated theoretically. According to previous experimental observations, a cleavage front overcomes the resistance of a high-angle grain boundary by first penetrating across it at a number of break-through points (BTP) and then separating apart persistent grain-boundary islands (PGBI). In the current study, this process is modeled as a competition between grain boundary shearing and crack front transmission. The numerical calculation shows that at a large grain boundary there exists an optimum BTP distance at which the grain boundary toughness is minimized, and when the BTP distance is relatively large its influence is secondary, fitting well with the experimental results.

© 2007 Elsevier B.V. All rights reserved.

*PACS:* 62.20.mm; 62.25.Mn; 61.72.Mm

*Keywords:* Grain boundary; Cleavage; Fracture toughness; Break-through mode

## 1. Introduction

Fracture toughness of engineering materials is an important issue in design of structures that work under adverse conditions [1]. In the framework of the well established linear elastic fracture mechanics (LEFM), it is usually assumed that in a brittle material there are a large number of pre-existing microcracks. Under an external loading, propagation of one or a few of them would lead to catastrophic failure [2]. The microcracks may be induced by residual stresses or unexpected thermal or mechanical loadings during processing and manufacturing. In a polycrystalline material, they are often assumed grain-sized. That is, a microcrack can be initiated either inside a grain or at a grain boundary; and once it propagates and encounters the first grain boundary, its tip would be arrested since grain boundary usually offers a higher resistance than a single crystal. Under this condition, the fracture resistance of

the material is actually determined by the grain boundary toughness.

In a recent experimental study, cleavage cracking processes across a number of high-angle grain boundaries in an iron–silicon alloy were examined in detail [3,4]. The difference between the grain boundary toughness and the toughness of a single crystal was attributed to the shift of fracture surface from the cleavage plane of one grain to that of the other, as well as the additional work required to separate grain boundary. It was observed that when the effective stress intensity at a crack tip was increased, the cleavage front would first penetrate across the boundary at a number of break-through points (BTP). The rest of the crack front in between the BTPs was left behind, arrested by persistent grain boundary islands (PGBI). The PGBI would be sheared apart once the penetration depth of the penetrating crack front reached a critical value. Since the cleavage planes in the two grains were of different orientations, the fracture surface across the grain boundary was sectioned, and further crack propagation would lead to formation of river markings.

\* Corresponding author.

*E-mail address:* [yqiao@ucsd.edu](mailto:yqiao@ucsd.edu) (Y. Qiao).

Clearly, the PGBI plays a critical role in the crack front transmission process [5–8]. Particularly, the crack trapping and bridging effects of PGBI are dominant, which is dependent on the PGBI width, or the distance between BTPs. One interesting phenomenon observed in fractography study was that along a large grain boundary the most probable distance between adjacent BTPs was 2–3  $\mu\text{m}$  for all the samples (see Fig. 1a), somewhat independent of the crystallographic orientations [3]. However, occasionally the BTP distance can be much larger, as shown in Fig. 1b, while BTP distance larger than 100  $\mu\text{m}$  have never been observed. When the BTP distance was large, it usually distributed quite uniformly in the range of 10–80  $\mu\text{m}$ . That is, the BTP distance distribution curve consisted of a peak at 2–3  $\mu\text{m}$  and a long, flat tail [3]. According to the river markings, in the large-BTP-distance area, the crack front penetrated all the BTPs nearly simultaneously, indicating that in this range the grain boundary resistance was insensitive to the BTP distance.

The lack of understanding of the factors governing BTP distance,  $w$ , has imposed considerable challenges to predicting grain boundary toughness. On the one hand, the most possible energetically favorable way for a crack to overcome PGBIs is to minimize  $w$ , i.e. the crack front should transmit from grain “1” into grain “2” simultaneously along the entire boundary, so that the area of grain

boundary involved in this process is negligible. On the other hand, there is no characteristic length of grain boundary structure in the range of 2–50  $\mu\text{m}$  [9]. In the past, in our discussions of grain boundary toughness,  $w$  was taken as a material constant. In the current work, through a theoretical analysis, we show that the characteristics of BTP distance distribution can be explained by the competition between crack front penetration and PGBI shearing.

## 2. Fracture resistance of persistent grain boundary islands

Fig. 2a depicts the cleavage cracking process across a high-angle grain boundary in a brittle material. The crack front first penetrates the boundary at the BTPs (“A” and “B”). As the penetration depth increases, the PGBI is sheared and thus the crack tip opens, as shown in Fig. 2b. The PGBI is left behind the verge of propagating, bridging across the fracture flanks, suppressing the crack advance through crack trapping effect. For the sake of simplicity, we analyze the crack trapping effect of a regular array of PGBI, where BTPs distribute along the grain boundary periodically. Without losing generality, assume that the crack is in a double-cantilever-beam (DCB) specimen. The height of the DCB arms,  $h$ , is much smaller than the initial crack length,  $a_0$ , so that the problem can be discussed in the framework of basic beam theory [10]. It will be shown shortly that the sample geometry has little influence on the calculation result of grain boundary fracture resistance.

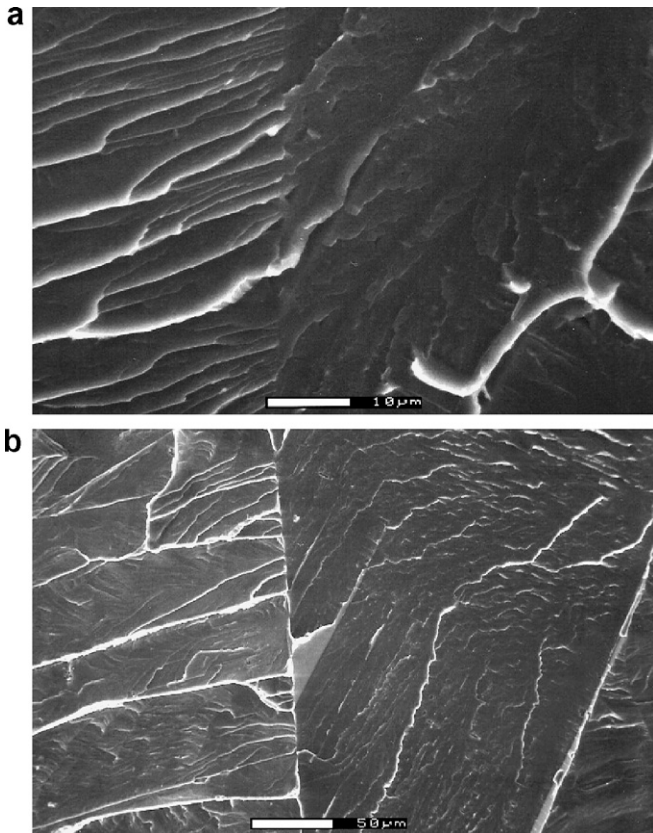


Fig. 1. SEM microscopy of cleavage cracking across a grain boundary in an iron–3 wt.% silicon alloy at different locations: (a) the distance between break-through points is smaller than a few microns; and (b) the distance between break-through points is 30–50  $\mu\text{m}$ . The crack propagated from the right to the left.

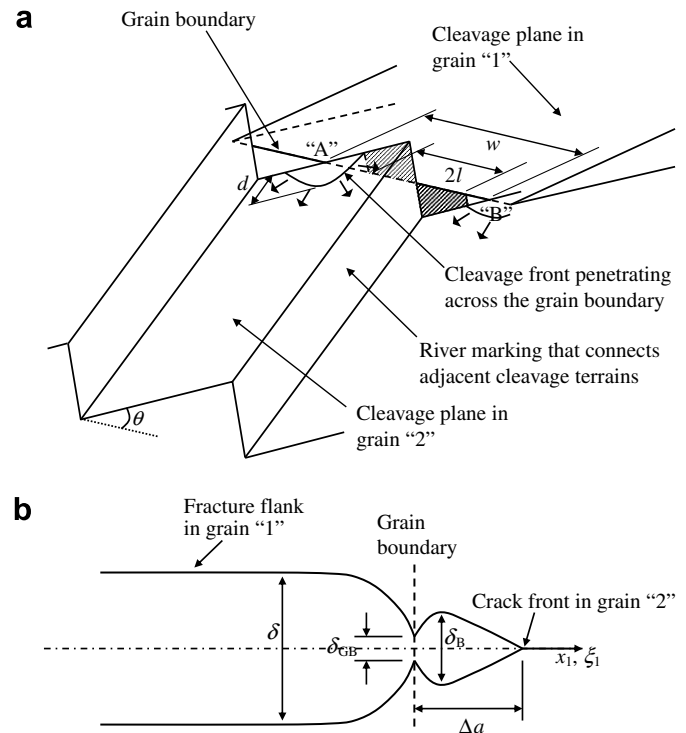


Fig. 2. Schematic diagrams of cleavage cracking across a high-angle grain boundary: (a) the three-dimensional view, where the crack propagates from the right to the left; (b) the side view, where the crack propagates from the left to the right.

With a pair of crack opening forces applied on the free end of the DCB specimen, the crack tip opening distance,  $\delta$ , increases, so does the energy release rate. Eventually, when the critical energy release rate,  $G_{bt}$ , is reached, the crack trapping effect of the PGBI array is overcome. In order to calculate  $G_{bt}$ , consider the case that ahead of the grain boundary there is a fracture resistance gradient,  $R(x_1)$ , which is always equal to the crack growth driven force,  $G(x_1)$ , and thus the crack growth is quasi-static, where  $\bar{x} = \{x_1, x_2\}$  is the coordinate system in the crack plane, with the origin at the initial cleavage front, subscript “1” indicating the axis along the crack growth direction, and “2” indicating the axis parallel to the initial crack front. Since the crack advance occurs after the grain boundary is overcome, this assumption would not affect the calculation of  $G_{bt}$ . During the crack growth, it is also assumed that the crack opening distance is constant. That is, we analyze a displacement controlled process.

At the initial crack front,

$$G(\hat{x} = 0) = R(\hat{x} = 0) = G_{bt}, \quad (1)$$

and at the final crack front

$$G(\hat{x} = \Delta a) = R(\hat{x} = \Delta a) = G_{ref}, \quad (2)$$

where  $\hat{x}$  is the total crack growth distance,  $\Delta a$  is the distance between the initial and the final cleavage fronts, and  $G_{ref}$  is the nominal fracture resistance of the second grain. If the cleavage plane in the first grain is parallel to the fracture surface, its resistance should be  $G_{cry}$ , the crystallographic resistance to cleavage crack advance of the material. The value of  $G_{ref}$  can be taken as  $G_{cry}/\cos\theta \cdot \cos\phi$ , where  $\theta$  and  $\phi$  are twist and tilt misorientation angles, respectively.

In a DCB sample, if the PGBI did not carry any load, the energy release rate can be calculated as [11]

$$G^*(\hat{x}) = \frac{3}{16} \frac{Eh^3 \Delta^2}{a^4}, \quad (3)$$

where  $a = a_0 + \hat{x}$  is the crack length,  $E$  is the Young's modulus,  $h$  is the height of DCB arm, and  $\Delta$  is the opening displacement. Combination of Eqs. (1) and (3) leads to

$$G^*(\hat{x}) = G_{bt}(1 + \hat{x}/a_0)^4, \quad (4)$$

which is equivalent to

$$K^*(\hat{x}) = \sqrt{\frac{E \cdot G^*(\hat{x})}{1 - \nu^2}} = \sqrt{\frac{E \cdot G_{bt}}{1 - \nu^2}} \left(1 + \frac{\hat{x}}{a_0}\right)^2, \quad (5)$$

where  $K^*$  is the effective stress intensity factor,  $\nu$  is the Poisson's ratio.

With the bridging stress in the PGBI being taken into consideration, the distribution of the stress intensity at the cleavage front at  $\hat{x}$  can be obtained as [12–14]

$$K(x_2, \hat{x}) = K^*(\hat{x}) + \int_{\Omega'} H(s, \bar{\xi}) \sigma(\bar{\xi}) d\bar{\xi}, \quad (6)$$

where  $\bar{\xi} = \{\xi_1, \xi_2\}$  indicates the global coordinate system;  $\Omega'$  denotes the intersection of PGBI with the crack plane,

which can be described as  $\xi_2 - n w \leq l$ , with  $2l$  being the PGBI width and  $n = 0, \pm 1, \pm 2 \dots$ .  $\sigma$  is the bridging stress distributed in  $\Omega'$ ; and  $H = \sqrt{2\hat{x}/\pi^3}/(s^2 + \xi_1^2)$ , with  $s = |x_2 - \xi_2|$ . The value of  $l$  is determined by  $(\sigma l) = \tau_{GB}$ , where  $\tau_{GB}$  is the shear strength of grain boundary. The average energy release rate can then be calculated as

$$G(\hat{x}) = \frac{1 - \nu^2}{E} \left[ \int_{-\infty}^{\infty} K(x_2, \hat{x}) dx_2 \right]^2. \quad (7)$$

In order to determine the bridging stress, the grain boundary shearing displacement,  $\delta_{GB}$ , must be taken into account. Once the crack trapping effect is overcome and the cleavage front propagates in the next grain, due to  $\sigma(\xi)$ , the PGBI would undergo a shear deformation. Since the material is brittle, the deformation should be elastic, i.e.

$$\sigma = \mu\gamma, \quad (8)$$

where  $\gamma$  is the effective shear strain and  $\mu$  is the shear modulus. Hence, the shear displacement of the PGBI is

$$\delta_{GB}(\bar{x}) = L \cdot \frac{\sigma(\bar{x})}{\mu} \quad (9)$$

with  $L = \delta_{GB}/\gamma$  being the effective thickness of PGBI. Note that the opening displacement of a crack subjected to bridging forces can be calculated as [15]

$$\delta(\bar{x}) = \frac{1 - \nu}{\mu} \left[ 2K^*(\hat{x}) \sqrt{\frac{\hat{x}}{2\pi}} \right] + \frac{1 - \nu}{\mu} \int_{\Omega'} \tilde{U}(\bar{x}, \bar{\xi}) \sigma(\bar{\xi}) d\bar{\xi}, \quad (10)$$

where

$$\tilde{U}(\bar{x}, \bar{\xi}) = \frac{1}{\rho\pi^2} \arctan \left\{ 2 \sqrt{\frac{x_1 \xi_1}{\rho^2}} \right\}$$

with  $\rho = \sqrt{(x_1 - \xi_1)^2 + (x_2 - \xi_2)^2}$  being the distance between  $\bar{x}$  and  $\bar{\xi}$ . Substitution of Eq. (9) into (10) gives

$$\frac{L \cdot \sigma(\bar{x})}{1 - \nu} = \left[ 2K^*(\hat{x}) \sqrt{\frac{\hat{x}}{2\pi}} \right] + \int_{\Omega'} \tilde{U}(\bar{x}, \bar{\xi}) \sigma(\bar{\xi}) d\bar{\xi} \quad \text{for } \bar{x} \text{ in } \Omega'. \quad (11)$$

By solving this integral equation, the bridging stress,  $\sigma$ , can be obtained.

The total fracture work associated with the crack growth from the initial front to the final front can now be calculated as

$$W = b \int_0^{\Delta a} G(\hat{x}) d\hat{x} + 2 \int_{\Omega'} \left[ \frac{L \cdot \delta(\bar{x})^2}{\mu} - \int_0^{\delta(\bar{x})} L(\delta/\mu) d\delta \right] d\bar{x}, \quad (12)$$

where  $b$  is the sample thickness. The first term at the right-hand side reflects the work of separation of crystallographic plane, and the second term captures the work of deformation of PGBI.

The fracture work must be balanced by the variation in strain energy  $U_i - U_a$ , with  $U_i$  and  $U_a$  being the strain energies before and after the crack growth, respectively. According to the basic beam theory, the calculation of  $U_i$  is quite straightforward:

$$U_i = \frac{Ebh^3 \Delta^2}{16a_0^3}, \quad (13)$$

which, when combined with Eq. (3), can be rewritten as

$$U_i = \frac{a_0 b}{3} G_{bt}. \quad (14)$$

The analysis of  $U_a$ , however, is more complicated, since the contribution of the bridging stress must be included. If the PGBI did not exist, the profile of the crack flank would be [15]

$$\delta_0(x_1) = 2 \frac{1-\nu}{\mu} K^*(\Delta a) \sqrt{\frac{\Delta a - x_1}{2\pi}}, \quad (15)$$

and the background strain energy would be

$$U_{as} = \frac{(a_0 + \Delta a)b}{3} G^*(\Delta a). \quad (16)$$

Based on Eq. (11), when the crack tip stops in the second grain, the bridging stress,  $\sigma_f$ , can be obtained by solving

$$\begin{aligned} \frac{L}{1-\nu} \cdot \frac{\sigma_f(\bar{x})}{\mu} &= \left[ 2K^*(\Delta a) \sqrt{\frac{\Delta a}{2\pi}} \right. \\ &\left. + \int_{\Omega'} \tilde{U}(\bar{x}, \bar{\xi}) \sigma(\bar{\xi}) d\bar{\xi} \right] \quad \text{for } \bar{x} \text{ in } \Omega'. \end{aligned} \quad (17)$$

This bridging stress would cause an additional strain energy in the matrix

$$U_{ap} = \int_{\Omega'} \sigma_f(\bar{x}) [\delta_0(x_1) - \delta(\bar{x})] d\bar{x}. \quad (18)$$

By substituting Eqs. (9) and (15) into (18), based on Eq. (16), we have

$$\begin{aligned} U_a &= \frac{(a_0 + \Delta a)b}{3} G^*(\Delta a) \\ &+ \int_{\Omega'} \sigma_f(\bar{x}) \left\{ 2 \frac{1-\nu}{\mu} K^*(\Delta a) \sqrt{\frac{\Delta a - x_1}{2\pi}} - L \cdot \frac{\sigma_f(\bar{x})}{\mu} \right\} d\bar{x}. \end{aligned} \quad (19)$$

Thus, the condition of energy equilibrium of crack growth can be expressed as

$$\begin{aligned} \frac{a_0 b}{3} G_{bt} - \frac{(a_0 + \Delta a)b}{3} G^*(\Delta a) \\ + \int_{\Omega'} \sigma_f(\bar{x}) \left\{ 2 \frac{1-\nu}{\mu} K^*(\Delta a) \sqrt{\frac{\Delta a - x_1}{2\pi}} - L \cdot \frac{\sigma_f(\bar{x})}{\mu} \right\} d\bar{x} \\ = b \int_0^{\Delta a} G(\hat{x}) d\hat{x} + 2 \int_{\Omega'} \left[ \frac{L \cdot \delta(\bar{x})^2}{\mu} - \int_0^{\delta(\bar{x})} L(\delta/\mu) d\delta \right] d\bar{x}. \end{aligned} \quad (20)$$

In Eq. (20), there are two unknowns,  $\Delta a$  and  $G_{bt}$ , which can be related to each other by setting  $G(\Delta a)$  as  $G_{ref}$  (Eq. (2)); that is

$$\frac{1-\nu^2}{E} \left[ \int_{-\infty}^{\infty} K(x_2, \Delta a) dx_2 \right]^2 = G_{ref}. \quad (21)$$

The governing equations are now complete. By solving Eqs. (20) and (21),  $\{G_{bt}, \Delta a\}$  can be calculated numerically. Since in the final equations the factors of  $b$  and  $h$  do not exist, the calculated  $G_{bt}$  was independent of the sample geometry. Note that, due to the assumption of the fracture resistance gradient, the calculated  $\Delta a$  does not reflect the actual crack growth length.

In the framework of the line average model that was initially developed by Rose [16] and Ortiz and Bower [17] for cleavage fracture in composite materials, the grain boundary resistance can be regressed as

$$\frac{G_{bt}}{G_{ref}} = \left( 1 - \frac{2l}{w} \right) + \left[ \alpha_1 + \alpha_2 \frac{2l}{w} + \alpha_3 \left( \frac{2l}{w} \right)^2 \right] \frac{2l}{w}, \quad (22)$$

where  $\alpha_1$ ,  $\alpha_2$ , and  $\alpha_3$  are parameters to be determined. By assuming that the BTP width follows a power-law function, we have  $2l = w - \beta_1 w^{\beta_2}$ , where  $\beta_1$  and  $\beta_2$  are two unknown parameters. Consequently,

$$\frac{G_{bt}}{G_{ref}} = \beta_1 w^\beta + (\alpha + \tilde{\alpha} w^\beta + \hat{\alpha} w^{2\beta})^2 (1 - \beta_1 w^\beta), \quad (23)$$

where  $\alpha = \alpha_1 + \alpha_2 + \alpha_3$ ,  $\tilde{\alpha} = -\alpha_2 \beta_1 - 2\alpha_3 \beta_1$ ,  $\hat{\alpha} = \alpha_3 \beta_1^2$ , and  $\beta = \beta_2 - 1$ . Using the Ritz method, Eq. (11) was enforced at the tenth points of a representative BTP. The numerical integration along the boundary was performed between  $\pm n w$ . It was found that when  $n = 5$ , further increase in  $n$  would not cause significant changes in numerical result of  $G_{bt}$ , i.e. the solution converged. The Poisson's ratio was taken as 0.28; the initial crack length was 100  $\mu\text{m}$ , the same as that in the experiment [3];  $L$  was taken as 5  $\text{nm}$ ; the Young's modulus,  $E$ , and the yield strength,  $Y$ , were set to 210 GPa and 250 MPa [3], respectively;  $\mu = E/\sqrt{3}$ ;

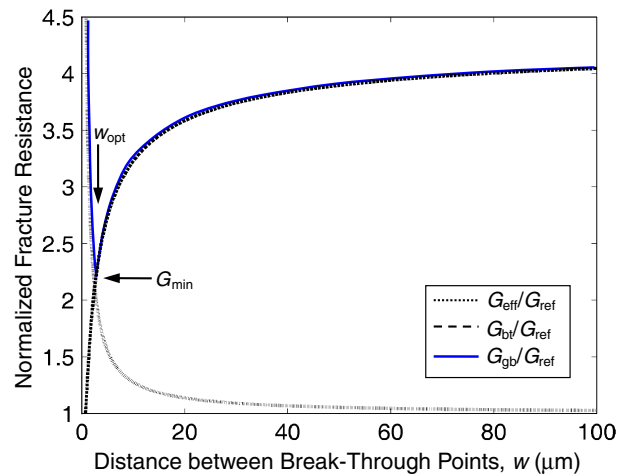


Fig. 3. The competition between  $G_{bt}$  and  $G_{eff}$ .

and  $\tau_{GB} = Y/\sqrt{3}$ . The value of  $L$  was somewhat arbitrarily chosen. It was noticed that as long as it was smaller than  $10 \mu\text{m}$ , the change in  $G_{bt}$  caused by its variation was less than 2%. By using these parameters, the integral equations could be transformed to a set of algebra equations, solving which gave the values of the parameters in Eq. (23):  $\beta_1 = 0.8$ ,  $\beta = -0.6$ ,  $\alpha = 4.35$ ,  $\tilde{\alpha} = -2.24$ , and  $\hat{\alpha} = 0.032$ . The normalized  $G_{bt}$  is shown as the dashed line in Fig. 3.

### 3. Continuous crack propagation across grain boundary

After the crack trapping effect associated with PGBI shearing is overcome, the crack can propagate forward in the grain ahead of the boundary. From the fracture surfaces shown in Fig. 1, it can be seen that in grain “2” river markings are generated as the crack advances. This process is depicted in Fig. 4. Due to the shift in cleavage plane across the grain boundary, the crack front branches into a number of sections. They propagate somewhat independently on a set of parallel terraces. The terraces must be bent and eventually be sheared apart to complete the separation of fracture surfaces, leading to the formation of a process zone behind the propagating front. Based on the classic Andersson-Bergkvist model [18], the effective fracture resistance can be assessed as

$$\frac{G_{\text{eff}}}{G_{\text{ref}}} = 1 + \frac{Y\delta_B^2}{2\sqrt{3} \cdot wG_{\text{ref}}}, \quad (24)$$

where  $\delta_B$  is the critical crack opening displacement (CCOD) at which the terraces are separated. The first term at the right-hand side captures the work of separation, and the second term captures the work of bending. According to experimental measurement of roughness of fracture surfaces,  $\delta_B$  was about  $2.7 \mu\text{m}$  [3]. Thus,  $G_{\text{eff}}/G_{\text{ref}}$  can be calculated as a function of  $w$ , and a typical curve is shown by the dotted line in Fig. 3, where  $G_{\text{cry}}$  is taken as the experimental result of  $164 \text{ J/m}^2$  [19] and both  $\theta$  and  $\phi$  are set to  $20^\circ$ , close to the middle point of their possible range ( $0$ – $45^\circ$ ). It will be

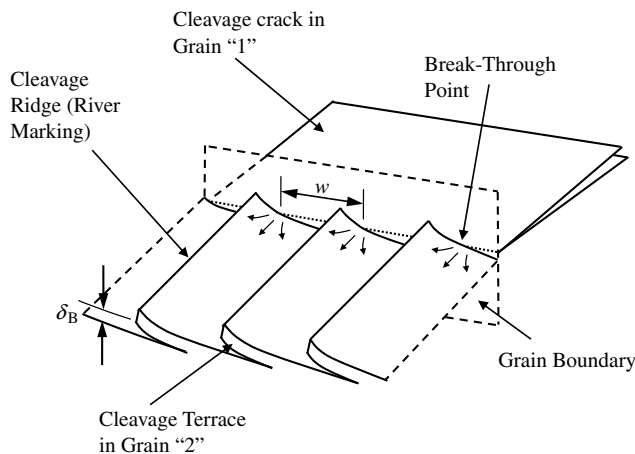


Fig. 4. A schematic diagram of bending and separation of cleavage terraces in the grain ahead of the grain boundary. The crack propagates from the right to the left.

shown shortly that the values of  $\theta$  and  $\phi$  do not have pronounced influence on  $w$ .

### 4. Discussion

Fig. 3 shows that, as the BTP distance,  $w$ , becomes larger, the crack trapping resistance of PGBI,  $G_{bt}$ , rises monotonically, while the resistance associated with the continuous crack propagation in the second grain,  $G_{\text{eff}}$ , keeps decreasing. There exists a critical value of  $w$ ,  $w_{\text{opt}}$ , at which  $G_{bt} = G_{\text{eff}}$ . When  $w$  is larger than  $w_{\text{opt}}$ ,  $G_{bt} > G_{\text{eff}}$ ; otherwise  $G_{bt} < G_{\text{eff}}$ . As a crack front encounters a grain boundary, the cleavage front penetrates across the boundary at the BTPs. Initially, since the BTPs distribute along the grain boundary randomly, they can be far and few between, leading to a large  $w$  value. As a result, the crack growth driving force,  $G$ , must be quite high to reach  $G_{bt}$ . Under this condition, if the crack trapping effect is overcome the crack would advance continuously since the resistance offered by the second grain,  $G_{\text{eff}}$ , has already been exceeded. If the crack growth driving force is smaller than  $G_{bt}$ , the front cannot transmit across the boundary. As  $G$  rises, more and more sections of cleavage front penetrate through the grain boundary, leading to the formation of new BTPs, and thus  $w$  is reduced. Consequently,  $G_{bt}$  decreases. However, when the BTP distance is lowered to smaller than  $w_{\text{opt}}$ , while  $G_{bt}$  would keep decreasing, it is no longer the dominant factor. In this case, even when the crack trapping effect of PGBI is overcome, the crack still cannot advance since the resistance of the second grain is larger, due to the high density of river markings. After the crack growth driving force exceeds  $G_{bt}$ , it must be further increased to  $G_{\text{eff}}$ . That is, the effective grain boundary fracture resistance,  $G_{\text{gb}}$ , should be taken as the larger one of  $G_{\text{eff}}$  and  $G_{bt}$ . When  $w < w_{\text{opt}}$ ,  $G_{\text{gb}} = G_{\text{eff}}$ ; when  $w > w_{\text{opt}}$ ,  $G_{\text{gb}} = G_{bt}$ :

$$G_{\text{gb}} = \max\{G_{\text{eff}}, G_{bt}\} = \begin{cases} G_{\text{eff}} & \text{when } w \leq w_{\text{opt}}, \\ G_{bt} & \text{when } w > w_{\text{opt}}, \end{cases} \quad (25)$$

as shown by the solid line in Fig. 3. At  $w_{\text{opt}}$ , the overall grain boundary resistance reaches the minimum value,  $G_{\text{min}}$ . The value of  $w_{\text{opt}}$  is around  $2$ – $3 \mu\text{m}$ , fitting well with the modal values of BTP distance distribution curves measured in experiment [3]. When  $w$  is either smaller than or larger than this value, the grain boundary offers a higher resistance, and the crack front transmission would be relatively energetically unfavorable.

The value of  $G_{\text{min}}$  is about 2.2 times of  $G_{\text{ref}}$ , comparable with but smaller than the experimental results, which were about 3.17 times larger than  $G_{\text{ref}}$  [4]. This should be attributed to the fact that in real specimens the BTP distances were not constant; rather,  $w$  could deviate from  $w_{\text{opt}}$  by an order of magnitude, resulting in larger values of  $G_{\text{gb}}$ . The variance in  $w$  can be caused by the kinetics of crack front transmission. For instance, if the formation rate of BTPs is smaller than the increase rate of crack growth driven force,  $G$  can reach a relatively high level of  $G_{bt}$  before sufficient BTPs

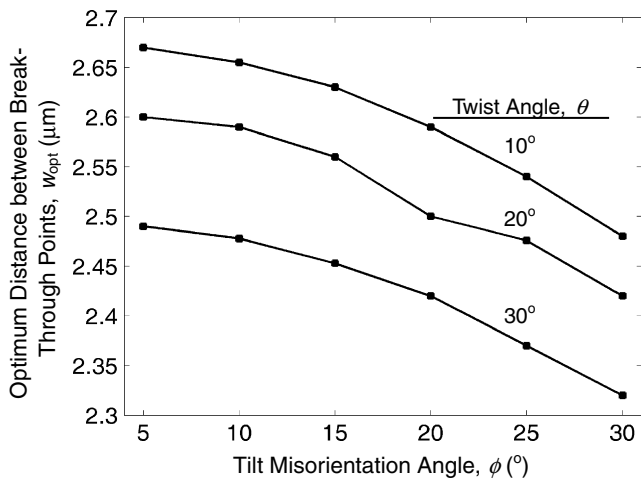


Fig. 5. The relationship between the break-through point distance and the crystallographic misorientation angles.

are developed. For another example, if the crack front penetrates across the boundary at a large number of BTPs even when  $G$  is still small, since BTPs do not vanish,  $G_{\text{eff}}$  would eventually be dominant and the overall grain boundary resistance is higher than  $G_{\text{min}}$ . Both cases have been observed in fracture experiments, as shown in Fig. 1. Only when the BTP formation and the  $G$  increase are balanced, can the BTP distance be stabilized at  $w_{\text{opt}}$  and  $G_{\text{gb}} \approx G_{\text{min}}$ .

When the BTP distance is relatively large, according to Fig. 3 the slope of the  $G_{\text{gb}}-w$  curve is much smaller than that in the small  $w$  range, i.e. the overall grain boundary fracture resistance is quite insensitive to  $w$ , which is consistent with the testing result that the BTP distance distribution curve is broad and flat in the range of  $w$  of 10–80  $\mu\text{m}$  [3]. Therefore, in a real specimen, if no sufficient BTPs can be formed, a small variation in local stress intensity, e.g. caused by the jerky profile of the boundary, would lead to a large difference in  $w$ .

Since both  $G_{\text{eff}}$  and  $G_{\text{bt}}$  are dependent on the crystallographic misorientation angles, the optimum BTP distance is also related to  $\theta$  and  $\phi$ . Fig. 5 shows that as the twist angle and the tilt angle increase,  $w_{\text{opt}}$  tends to decrease. However, this change is quite small even when  $\theta$  and  $\phi$  vary across most of their possible ranges. In all the investigated cases,  $w_{\text{opt}}$  is around 2.5  $\mu\text{m}$ , in agreement with the experimental observation that no matter how different the crystallographic orientations were there was no detectable variation in BTP distance distribution [3]. Hence,  $w_{\text{opt}}$  can be regarded as a grain boundary constant, independent of the properties of adjacent grains.

## 5. Conclusions

In the current study, we show that when the cleavage front transmission process across a high-angle grain boundary is modeled as a competition between the shearing of persistence grain boundary islands and the continuous front propagation in the grain ahead of the boundary, the

observed experimental results can be well explained. The overall grain boundary toughness is determined by the crack trapping effect and the bending of cleavage terraces, both of which are dependent on the distance between break-through points. The following conclusions are drawn:

- (1) There exists an optimum break-through point distance at which the overall grain boundary fracture resistance reaches the minimum value.
- (2) When the distance between break-through points is relatively small, the grain boundary fracture resistance is governed by the river marking behaviors in the grain ahead of the boundary; when the distance is relatively large, the crack trapping effect of the grain boundary is dominant.
- (3) When the break-through point distance is close to the optimum value, its influence on the grain boundary resistance is pronounced; when the number of break-through points is insufficient, a small variation in local stress intensity can cause a large change in appearance of fracture surface, while the change in grain boundary toughness is relatively small.
- (4) The optimum break-through point distance is insensitive to the crystallographic orientations, and therefore may be regarded as a grain boundary constant.

## Acknowledgement

This work was supported by the US Department of Energy, Office of Basic Energy Sciences under Contract DE-FG02-07ER46355.

## References

- [1] T.L. Anderson, Fracture Mechanics: Fundamentals and Applications, CRC Press, 2004.
- [2] R.J. Sanford, Principles of Fracture Mechanics, Prentice Hall, 2002.
- [3] Y. Qiao, A.S. Argon, Mech. Mater. 35 (2003) 313–331.
- [4] Y. Qiao, A.S. Argon, Mech. Mater. 35 (2003) 129–154.
- [5] X. Kong, Y. Qiao, Fatigue Fract. Eng. Mater. Struct. 28 (2005) 753–758.
- [6] S.S. Chakravarthula, Y. Qiao, Int. J. Fatigue 27 (2005) 1251–1254.
- [7] Y. Qiao, X. Kong, Met. Mater. Int. 12 (2006) 27–30.
- [8] Y. Qiao, Mater. Sci. Eng. A 361 (2003) 350–357.
- [9] P.E.J. Flewitt, R.K. Wild, Grain Boundaries: Their Microstructures and Chemistry, John Wiley & Sons, 2001.
- [10] R.W. Hertzberg, Deformation and Fracture Mechanics of Engineering Materials, Wiley, 1995.
- [11] A. Shukla, Practical Fracture Mechanics in Design, CRC Press, 2004.
- [12] G. Xu, A.F. Bower, M. Ortiz, J. Mech. Phys. Solids 46 (1998) 1815–1833.
- [13] T.M. Mower, A.S. Argon, Mech. Mater. 19 (1995) 343–364.
- [14] A.F. Bower, M. Ortiz, Trans ASME 115 (1993) 228–236.
- [15] Y.S. Ulfyand, Survey of Articles on the Application of Integral Transforms in Theory of Elasticity, University of North Carolina, Raleigh, NC, 1965.
- [16] L.R.F. Rose, Mech. Mater. 6 (1987) 11–15.
- [17] A.F. Bower, M. Ortiz, J. Mech. Phys. Solids 39 (1991) 815–858.
- [18] H. Andersson, H. Bergkvist, J. Mech. Phys. Solids 18 (1970) 1–28.
- [19] Y. Qiao, A.S. Argon, Mech. Mater. 35 (2003) 903–912.